

# Results on pilot plant SRF oxy-fuel combustion demonstration

Author: Joseba Moreno, Max Schmid

Release Status: FINAL

Date: 23 May 2022

Filename and version: NEWEST\_D3.2.2\_USTUTT



ACT2 NEWEST-CCUS project No 299683

This project NEWEST-CCUS is funded through the ACT programme (Accelerating CCS Technologies, Horizon2020 Project No 294766). Financial contributions made from The Research Council of Norway, (RCN), Norway; Bundesministerium für Wirtschaft und Energie (BMWi), Germany; Netherlands Ministry of Economic Affairs and Climate Policy, the Netherlands; and Department for Business, Energy & Industrial Strategy (BEIS) together with the Natural Environment Research Council (NERC) and the Engineering and Physical Sciences Research Council (EPSRC), United Kingdom are gratefully acknowledged.



This work has been jointly supported by the German Federal Ministry of Economic Affairs and Climate Action (BMWK) under Grant No. 03EE5020.



# Document History

## Location

This document is stored in the following location:

Filename	NEWEST_D3.2.2_USTUTT
Location	SCCS shared drive


## Revision History

This document has been through the following revisions:

Version No.	Revision Date	Filename/Location stored:	Brief Summary of Changes
Version 1	23/05/2022	NEWEST_D3.2.2_USTUTT	

## Authorisation

This document requires the following approvals:

AUTHORISATION	Name	Signature	Date
WP Leader or co-leader	Mario Ditaranto, Max Schmid		
Project Coordinator	Mathieu Lucquiaud		29/11/2022

## Distribution

This document has been distributed to:

Name	Title	Version Issued	Date of Issue
			00/00/0000

© NEWEST-CCUS project, 2020

No third-party textual or artistic material is included in the publication without the copyright holder's prior consent to further dissemination by other third parties.

Reproduction is authorised provided the source is acknowledged.

### **Disclaimer**

The information and views set out in this deliverable are those of the author(s) and do not necessarily reflect the official opinion of the Funders (RCN, BMWi, RVO, BEIS with NERC and EPSRC). Neither the Funders and bodies nor any person acting on their behalf may be held responsible for the use which may be made of the information contained therein.

# Executive Summary

Within the NEWEST-CCUS project (Project-Nr.: 299683), different carbon capture, usage, and storage (CCUS) technologies are to be investigated in the context of Waste-to-Energy (WtE) plants, aiming at achieving net-negative CO<sub>2</sub> emissions.

Oxy-fuel combustion of refuse waste is gaining considerable attention as a viable CO<sub>2</sub> negative technology that can enable the continued use of stationary combustion plants during the transition to renewable energy sources. Compared to fossil fuels, waste-derived fuels tend to be highly heterogeneous and to contain a greater amount of alkaline metals and chlorine. Therefore, experimental studies are mandatory to thoroughly elucidate refuse materials' combustion and pollutant formation behavior.

This deliverable presents an experimental investigation on the air and oxy-fuel combustion of solid recovered fuel at a 200 kW<sub>th</sub> circulating fluidized bed facility. In the course of three experimental campaigns, the effects of combustion atmosphere and temperature on pollutant formation (i.e., NO<sub>x</sub>, SO<sub>2</sub>, and HCl) and reactor hydrodynamics were systematically studied. In contrast to air-firing conditions, the experimental results showed that oxy-fuel combustion enhanced the volume concentration of NO<sub>x</sub> by about 50% while simultaneously decreasing the fuel-specific NO<sub>x</sub> emissions (by about 33%). The volume concentrations of SO<sub>2</sub> and HCl were significantly influenced by the absorption capacity of calcium-containing ash particles, yielding corresponding values close to 10 and 200 ppmv at 871–880 °C under oxy-fuel combustion conditions. In addition, the analysis of hydrodynamic data revealed that smooth temperature profiles are indispensable to mitigate bed sintering and agglomeration risks during oxy-fuel operation.

The results included in this report provide a valuable contribution to the database of experimental information on the oxy-fuel combustion of alternative fuels, which can be applied in future process model validations and scale-up studies.

# Table of Contents

<b>Executive Summary</b> .....	<b>4</b>
<b>List of abbreviations</b> .....	<b>6</b>
<b>List of symbols</b> .....	<b>6</b>
<b>1 Introduction</b> .....	<b>8</b>
<b>2 The oxy-fuel technology for CO<sub>2</sub> capture</b> .....	<b>8</b>
<b>3 Experimental section</b> .....	<b>9</b>
4.1 The 200 kW <sub>th</sub> oxy-CFBC facility .....	9
4.2 Fuel and bed material.....	10
<b>4 Results and discussion</b> .....	<b>11</b>
4.1 Gaseous emissions .....	11
4.1.1 Carbon monoxide (CO).....	11
4.1.2 Nitrogen oxides (NO <sub>x</sub> ) .....	12
4.1.3 Acidic gases (SO <sub>2</sub> and HCl).....	14
4.2 Hydrodynamic behavior .....	15
4.3 Operation at increased oxy-fuel levels .....	16
<b>5 Conclusions</b> .....	<b>17</b>
<b>Acknowledgements</b> .....	<b>18</b>
<b>References</b> .....	<b>18</b>

## List of abbreviations

Acronym	Description
ad	air-dried
ASU	Air Separation Unit
BECCS	Bio-energy combined with Carbon Capture and Storage
BFB	Bubbling Fluidized Bed
CCS	Carbon Capture and Storage
CFB	Circulating Fluidized Bed
CPU	CO <sub>2</sub> Compression and Purification Unit
FG	Flue Gas
in	inlet
out	outlet
SRF	Solid Recovered Fuel
waf	water-ash-free
wf	water-free
WtE	Waste-to-Energy
th	thermal
TRL	Technology Readiness Level

## List of symbols

Symbol	Description
$c_i$	Mass fraction of component "i" in gas (mg/m <sup>3</sup> )
$e_i$	Emission factor of component "i" (mg/MJ <sub>th</sub> )
$h$	Height (m)
$t$	Time (h)

$T$	Temperature (°C)
$\dot{V}$	Volume flow (m <sup>3</sup> /h, STP)
$x_i$	Mass fraction of component “i” in sorbent (kg/kg)
$y_i$	Volume fraction of component “i” in gas (vol% or ppmv)
$\eta_i$	Conversion ratio of component “i” (kg/kg)
$\Delta p$	Pressure difference (mbar)
$\gamma_i$	Mass fraction of component “i” in fuel (kg/kg)
$\nu_{recycled}$	Flue gas recirculation rate (%)
$\xi$	Stoichiometric oxygen-to-fuel ratio (kg/kg)



## 1 Introduction

Climate change mitigation and sustainable waste management are among the most important societal challenges recognized by the 2015 Paris Climate Agreement [30] and the European Union Action Plan for a Circular Economy Package [8]. The thermal valorization of refuse waste (e.g., incineration and co-combustion) has gained increasing popularity in recent years as a solution for decreasing the volume of solids disposed of in landfills, and thereby the associated greenhouse gas emissions. Still, the intrinsic fuel characteristics (e.g., form and particle size, ash and moisture content) must be carefully evaluated during the process design step to ensure reliable plant operation and effective emissions control.

Due to their high fuel adaptability, increased solid residence time, and low pollutant emission, circulating fluidized bed (CFB) systems are particularly well-suited for the combustion of low-grade fuels. Moreover, CFB systems can be applied within the framework of carbon capture and storage (CCS) technologies to capture CO<sub>2</sub> from power and industrial sources. In parallel, the combination of CCS with non-conventional fuels enables the achievement of net negative emissions by sequestration of biogenic CO<sub>2</sub>. The latter approach is often referred to as bioenergy with carbon capture and storage (BECCS) and is expected to play a major role in meeting the 2050 zero-carbon emissions target [3,6,9,30,31].

## 2 The oxy-fuel technology for CO<sub>2</sub> capture

In the last decades, oxy-fuel CFB combustion has evolved into one of the leading technologies considered for capturing CO<sub>2</sub> from power plants with CCS. The process consists of burning fuel with nearly pure oxygen instead of air. The justification for using oxy-fuel is to generate a flue gas with a high concentration of CO<sub>2</sub> and water vapor and then separate the CO<sub>2</sub> from the flue gas by dehydration and low-temperature purification processes. Consequently, the oxy-fuel combustion for power generation typically consists of the following major units: (i) an air separation unit (ASU) for oxygen production; (ii) a boiler or gas turbine for combustion of fuel and generation of heat; and (iii) a CO<sub>2</sub> processing unit (CPU) for final purification of the CO<sub>2</sub> prior to utilization or storage. With the purpose of controlling the flame temperature, part of the flue gas is recycled back into the boiler. In addition, the process offers the possibility to comprehensively reduce the amount of SO<sub>x</sub> in the flue gas and mitigate adverse effects such as slagging and fouling in heat exchanger surfaces. The latter is achieved by continuous addition of sorbents (e.g., limestone) and additives (e.g., aluminosilicates), respectively.

Besides, oxy-fuel combustion may affect the emissions of particular gas pollutants. As compared with air-firing, oxy-fuel tends to increase the volume concentration of NO<sub>x</sub> in the flue gas while simultaneously reducing the mass of NO<sub>x</sub> released per energy generated [10,13]. Besides, the furnace temperature is another major condition affecting NO<sub>x</sub> formation during oxy-fuel combustion. Thermal NO<sub>x</sub> formation is greatly suppressed in oxy-CFB boilers due to the moderate combustion temperature and staged oxidant addition [15,22]. However, elevated oxy-fuel levels might promote thermal NO<sub>x</sub> formation due to the presence of localized hot spots resulting from the more intense combustion conditions [28].

HCl is another critical component in utility boilers using alternative fuels, as elevated emissions of HCl are well-known to cause major operational issues such as slagging, fouling, and corrosion [26]. At high temperatures, alkali metals (M) and chlorine (Cl) are released from the fuel into the flue gas as vaporized alkali metal chlorides (MCl). In the following, the sulfation process transforms alkali

chlorides into alkali sulfates ( $M_2SO_4$ ) under the effect of humid sulfur species, releasing chlorine as HCl [17].

This deliverable evaluates the combustion behavior of solid recovered fuel (SRF) under conditions prevailing in modern waste CFB incinerators. In this study, we evaluate the impact of combustion atmosphere (i.e., air and oxy-fuel) and temperature (i.e., 840-924 °C) on gaseous emissions (i.e.,  $NO_x$ ,  $SO_2$ , and HCl) and reactor hydrodynamics. Also, the feasibility of operating the system at increased oxy-fuel levels (up to 45 vol%  $O_2$ ) is demonstrated. The experiments were carried out at the University of Stuttgart's 200 kW<sub>th</sub> CFB pilot plant, under conditions typical of industrial operation (i.e., recirculated flue gas and technically pure oxygen). The evaluation of ash formation and deposition behavior is beyond the scope of this report.

### 3 Experimental section

#### 4.1 The 200 kW<sub>th</sub> oxy-CFBC facility

The 200 kW<sub>th</sub> pilot facility at the University of Stuttgart is composed of three fluidized bed reactors, which are connected by a solid flow transport system [11,19]. In the NEWEST-CCUS project only one of the reactors is used for the oxy-fuel validation tests. A scheme of the installation is shown in Figure 1.

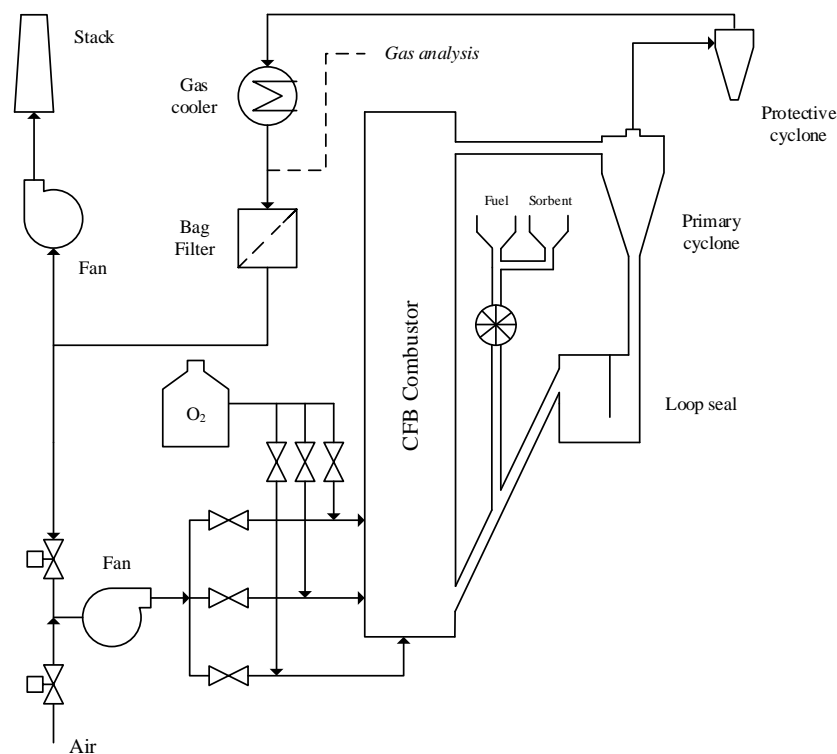


**Figure 1.** Schematic of the University of Stuttgart's 200 kW<sub>th</sub> oxy-fuel CFB combustion facility

The facility can be used for combustion or gas and solid fuels, applying air, oxygen enriched air or oxy-fuel operating conditions. Additionally, the CFB combustor can be coupled to the other CFB and bubbling fluidized bed (BFB) units for investigating pre-combustion and post-combustion  $CO_2$  capture possibilities.

Concerning the technical construction, the CFB reactor is 10 m high and has an average internal diameter of 20 cm. As fluidization gases air, oxygen or oxy-fuel gas can be applied. These are provided by a high-pressure blower and introduced at three different stages for a better control of temperature hotspots and NO<sub>x</sub> emissions. After the combustion chamber, the flue gas and the sorbent are separated by a high efficiency primary cyclone. The gas is then passed through a secondary cyclone and bagfilter for fine ash removal. After that, the flue gas can be either recirculated into the system or vented to the atmosphere by means of an ID-fan.

The combustion temperature can be regulated by 6 water cooled bayonet heat exchanger tubes, which can be inserted independently from the top of the riser. The fuel and the sorbent are gravimetrically controlled and continuously fed into the reactor bottom. The gas measurements of the combustion flue gas in the experimental facility are conducted between the gas cooler and the bag filter. All continuous gas measurements are carried out cold and dry. Additional gas species of interest (e.g. HCl) can be measured by a FTIR system. For a more detailed explanation of the experimental facility please refer elsewhere [20].

#### 4.2 Fuel and bed material

The chemical composition of the fuel utilized in this work is given in Table 1. The latter consists of high calorific fractions separated from bulky and household waste (SBS®1, REMONDIS GmbH & Co. KG, Region Rheinland, Germany) intentionally prepared to meet quality requirements such as calorific value and mercury or chlorine content [24]. To guarantee adequate SRF dosing in the pilot facility, a procedure for conditioning the SBS®1 was developed. The process consisted of mechanical steps such as shredding, briquetting, and subsequent shredding (see Figure 2). Besides, Table 2 shows the chemical composition of the bed material used in the pilot experiments. The silica sand DORSILIT® 9 was delivered from Gebrüder Dorfner GmbH & Co. Kaolin- und Kristallquarzsand-Werke KG in the size range of 100 – 400 µm.

**Table 1.** Chemical composition of the solid recovered fuel used in the pilot-scale experiments (waf: water-ash-free, wf: water-free, ad: air-dried)

Remondis SBS®1	$\gamma_C$	$\gamma_H$	$\gamma_O$	$\gamma_N$	$\gamma_S$	$\gamma_{Cl}$	$\gamma_{ash}$	$\gamma_{H_2O}$
	kg/kg, waf						kg/kg, wf	kg/kg, ad
	0.547	0.074	0.345	0.027	0.002	0.005	0.094	0.114

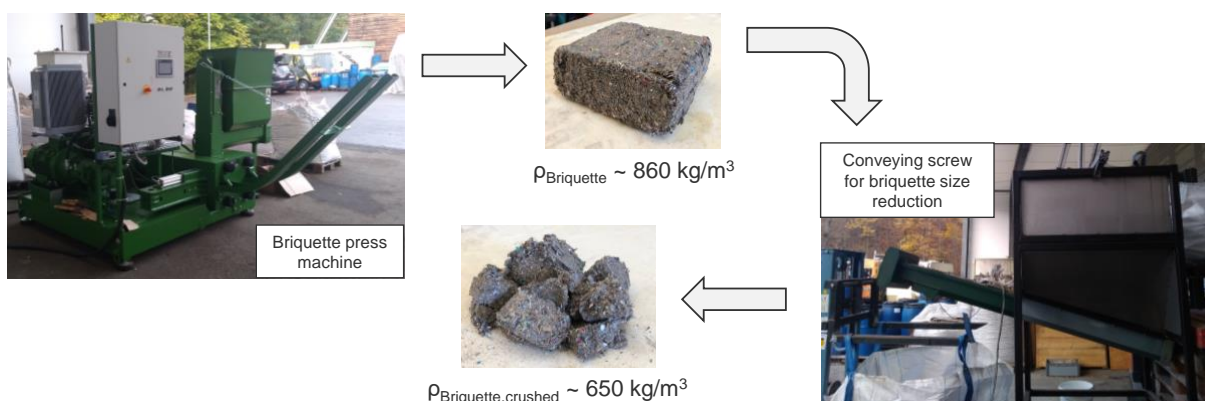


**Figure 2.** Conditioning of SBS®1 for pilot-scale experiments

**Table 2.** Chemical composition of the bed material used in the pilot-scale experiments (wf: water-free)

DORSILIT® 9	$x_{SiO_2}$	$x_{Al_2O_3}$	$x_{Fe_2O_3}$	$x_{K_2O}$	$x_{others}$
	kg/kg, wf				
	0.95	0.025	0.0004	0.023	0.0016

## 4 Results and discussion

In this deliverable we explore the CFB combustion characteristics of SRF under process conditions similar to those envisaged in modern waste incinerators. The results presented in this report are related to the CFB combustor’s performance under different oxidizing gas atmospheres and process temperatures, so as to derive implications on pollutant formation and hydrodynamic stability.

Each experiment was operated for at least one hour – although in general 2 hours – after steady-state conditions were reached. In addition, selected experiments were conducted for longer operational times to assess the process performance on a longer-term basis. In the course of the presented experiments, the pilot facility was operated over a wide of operation conditions [20]. While the reactor inventory was maintained roughly constant (i.e., 1005-1238 kg/m<sup>2</sup> or 32-39 kg), the process temperature was varied between 840-924 °C to derive implications on the overall process performance. During oxy-fuel combustion, two different inlet oxygen concentrations were mainly investigated, namely 28 vol% (OXY28) and 35 vol% (OXY35). Both oxy-fuel cases were established by adjusting the amount of recirculated flue gas, which averaged 87% and 74%, respectively. Furthermore, increased oxy-fuel levels (up to OXY45) have been demonstrated at the 200 kW<sub>th</sub> oxy-CFB combustion facility and will be discussed later on within this deliverable. Air-firing experiments yielded considerably higher superficial gas velocities (up to 6.5 m/s) due to the increased gas flow throughput. Nevertheless, the observed differences in superficial gas velocities posed a minor effect on the system’s hydrodynamics as stable and sufficient internal solid circulation could be attained in both operation modes. Besides, the oxidant staging level was kept constant in the course of the experimental investigations.

### 4.1 Gaseous emissions

Within a first phase of the data evaluation process, a general material balance is applied to the system using measured plant data such as gas concentrations, volume flows, and solid flows [20]. After successful closure of the material balance, gaseous emissions and concentrations are evaluated according to the methodology described in a recent publication [20].

#### 4.1.1 Carbon monoxide (CO)

The combustion conditions defined in a boiler have a crucial influence on the emissions of the diverse gas species. Complete combustion of biomass and waste-derived fuels (e.g., SRF) requires increased stoichiometric oxygen-to-fuel ratios to compensate for the relatively high volatile fraction and the large inhomogeneity of biogenic fuels [7,21]. The results presented in Figure 3 corroborate the last assertion. At the 200 kW<sub>th</sub> CFB combustion facility SBS®1 was combusted over a wide range of stoichiometric oxygen-to-fuel ratios both during air and oxy-fuel firing conditions. The results indicate that a minimum stoichiometric-to-fuel ratio of 1.4 is required in both cases to drive CO emissions below the mark of 100 mg/MJ<sub>th</sub>, which corresponds roughly to the emission limit of

250 mg/m<sup>3</sup> imposed on non-woody biofuel German combustion plants with a total capacity up to 100 MW [1].

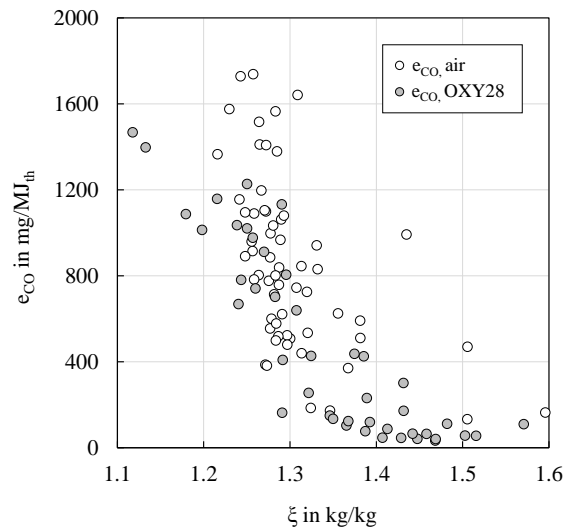


**Figure 3.** CO emission factor ( $e_{CO}$ ) vs stoichiometric oxygen-to-fuel ratio ( $\xi$ ) during air-firing and oxy-fuel combustion conditions [20]

#### 4.1.2 Nitrogen oxides (NO<sub>x</sub>)

Nitrogen oxides (NO<sub>x</sub>) represent a potential corrosion risk in the processing of CO<sub>2</sub> from oxy-fuel combustion processes due to the formation of nitric acid [25]. Figure 4 introduces the fuel-specific NO<sub>x</sub> emission factor (a) and the NO<sub>x</sub> volume concentration (b) against the stoichiometric oxygen-to-fuel ratio, both during air and oxy-fuel firing conditions.

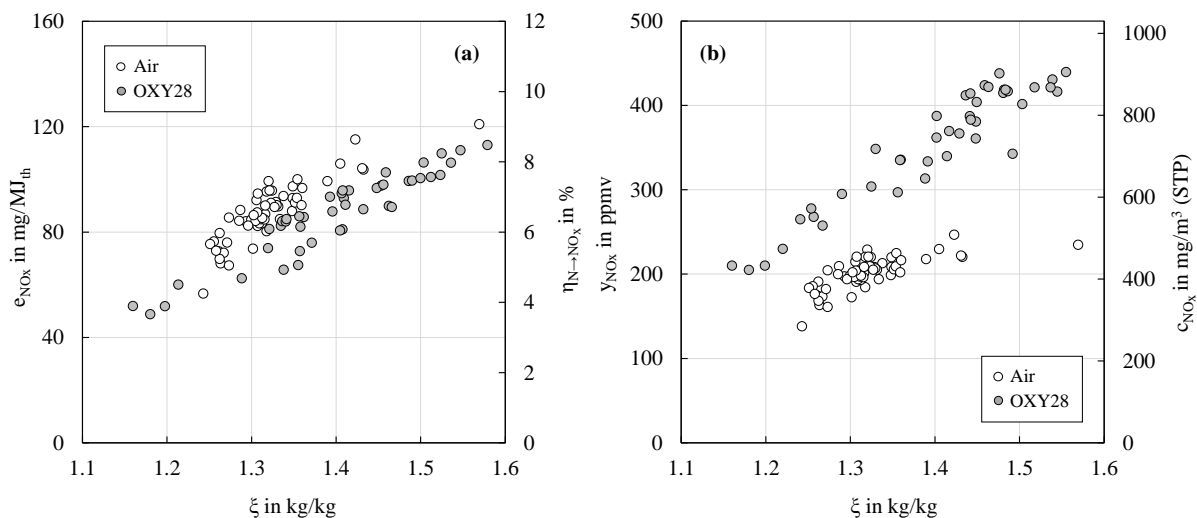


**Figure 4.** (a) NO<sub>x</sub> emission factor ( $e_{NO_x}$ ) and fuel-N to NO<sub>x</sub> conversion ratio ( $\eta_{N \rightarrow NO_x}$ ) vs stoichiometric oxygen-to-fuel ratio ( $\xi$ ). (b) NO<sub>x</sub> concentration ( $y_{NO_x}$ ,  $c_{NO_x}$ ) vs stoichiometric oxygen-to-fuel ratio ( $\xi$ ) [20]

The NO<sub>x</sub> concentration during oxy-fuel combustion tends to be higher than during air firing conditions due to (i) gas pollutants enrichment through flue gas recirculation and (ii) the increased amount of oxygen in the oxidizer. At the same time, fuel-specific NO<sub>x</sub> emissions are generally lower in the oxy-fuel case mainly because of (i) the low nitrogen environment in combination with (ii) the

reduction in the total flue gas flow. The findings of this study support both assertions. Figure 4a indicates that the mass of  $\text{NO}_x$  released per energy generated during oxy-fuel was up to 33% lower than during the air-combustion case. Concurrently, the  $\text{NO}_x$  volume fraction measured during oxy-fuel was about 50% higher than the  $\text{NO}_x$  concentration measured during air combustion conditions (see Figure 4b). An exemplary switch from air-firing to oxy-combustion conditions is displayed in Figure 5. Besides, the linear behavior of  $\text{NO}_x$  with excess oxygen can be attributed to a decreased reducing zone in the combustor, which results in the reduction of  $\text{NO}_x$  to  $\text{N}_2$  [23].

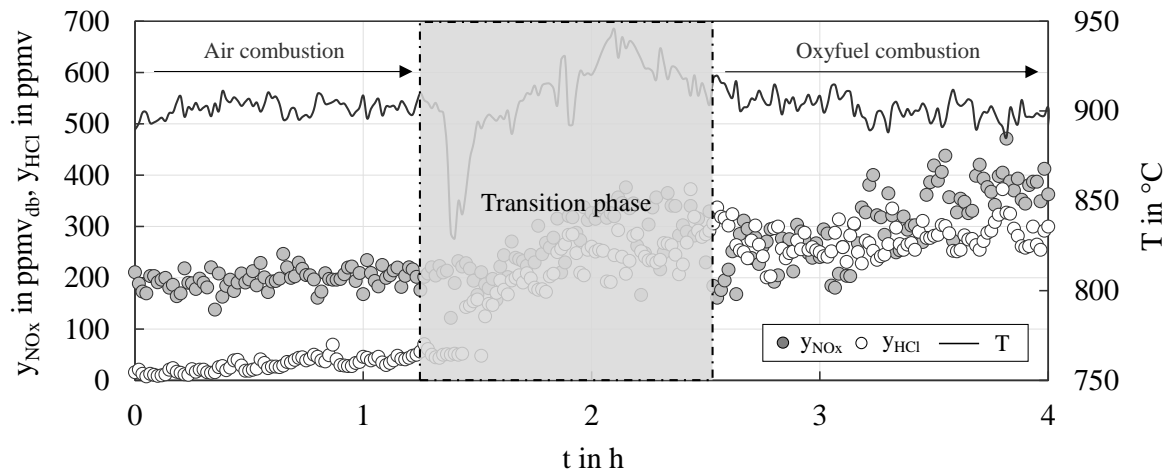


**Figure 5.** Switch from air-firing to oxy-combustion operation conditions. Influence on temperature ( $T$ ) and flue gas composition ( $y_{\text{NO}_x}$ ,  $y_{\text{HCl}}$ ).

The combustion temperature is another major variable that influences the fuel's conversion degree and, thus, the combustion flue gas composition. Figure 6 introduces the concentration of  $\text{NO}_x$  for all conducted experiments against the reactor temperature.

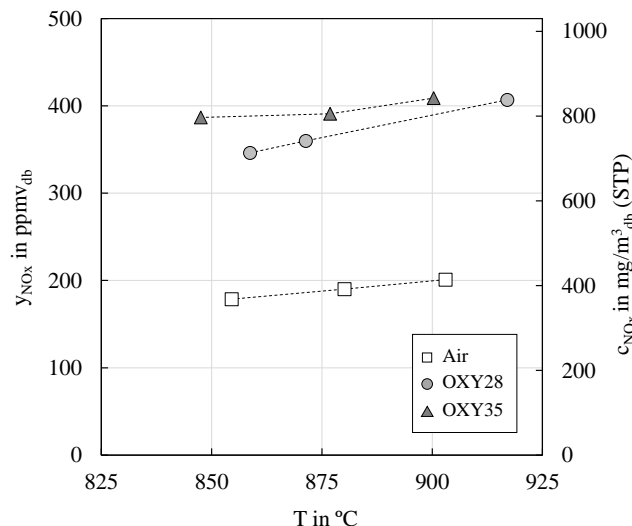


**Figure 6.**  $\text{NO}_x$  concentration ( $y_{\text{NO}_x}$ ,  $c_{\text{NO}_x}$ ) vs reactor temperature ( $T$ ) for all investigated air and oxy-fuel combustion experiments [20]

Compared to air-firing, the graph indicates that  $\text{NO}_x$  levels are substantially promoted during oxy-fuel combustion. With a target boiler temperature of 860 °C, 179 ppmv were measured during air-firing conditions. Concurrently, 346 ppmv were yielded at an inlet oxygen concentration of 28 vol%

and a similar temperature. Within the same combustion setting, the reactor temperature showed a marginal influence on  $y_{NO_x}$ , indicating a slightly increasing tendency in all investigated cases [29].

#### 4.1.3 Acidic gases (SO<sub>2</sub> and HCl)

Generally, biomass and fuels with increased biogenic share (e.g., SRF) are characterized by a lower sulfur content than most coals, reducing fuel-related SO<sub>2</sub> emissions responsible for acidification [16,18]. However, the sulfur amount in the fuel can play an essential role in sulfating alkali chlorides, which are known for enhancing deposit formation and accelerating superheater corrosion.

##### 4.1.3.1 Sulfur dioxide (SO<sub>2</sub>)

The influence of combustion atmosphere (a) and process temperature (b) on the evolution of SO<sub>2</sub> and HCl concentrations is introduced in Figure 7 and Figure 8, respectively. Figure 7a indicates that SO<sub>2</sub> emissions tend to decrease with increasing  $\xi$  (i.e., fuel-rich region) and might be attributed to alkali species in ash that favor sulfur retention [4]. In parallel, Figure 7b presents the dependency of SO<sub>2</sub> volume concentration from the process temperature. According to the illustration, there is a temperature range in which SO<sub>2</sub> is remarkably suppressed. The latter behavior can be explained by the presence of calcium-containing species in the fuel ash, which can bind SO<sub>2</sub> according to different routes [27]. Moreover, the proposed temperature range in this study (i.e., 871 – 880 °C) correlates well with the observations made by Díez et al., who reported maximum SO<sub>2</sub> retention values when operating in a temperature window between 880-890 °C [5].

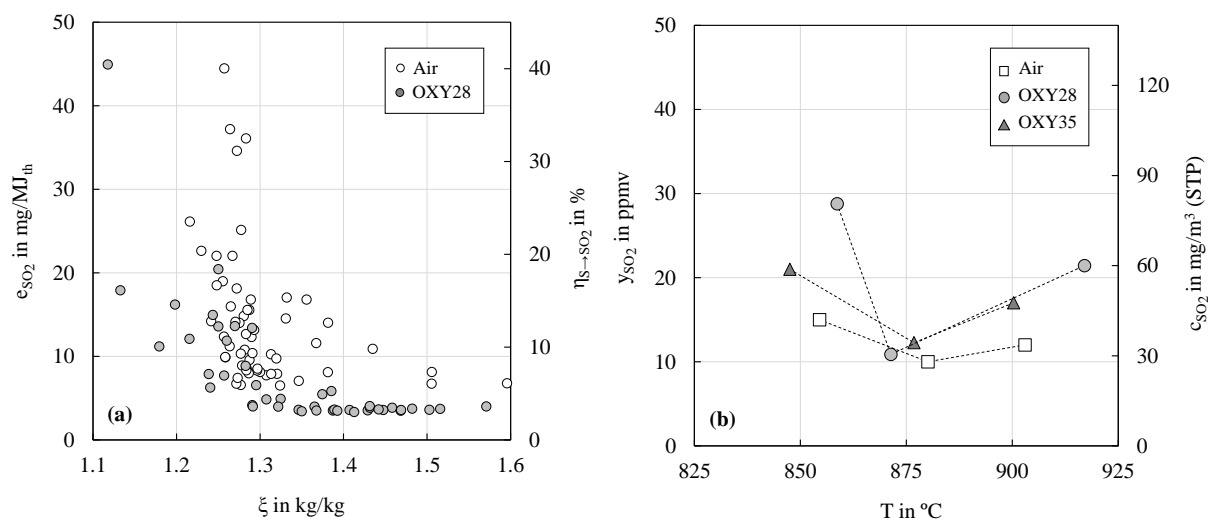


**Figure 7.** (a) SO<sub>2</sub> emission factor ( $e_{SO_2}$ ) and fuel-S to SO<sub>2</sub> ratio ( $\eta_{S \rightarrow SO_2}$ ) vs stoichiometric oxygen-to-fuel ratio ( $\xi$ ). (b) SO<sub>2</sub> concentration ( $y_{SO_2}$ ,  $c_{SO_2}$ ) vs reactor temperature ( $T$ ) [20]

##### 4.1.3.2 Hydrogen chloride (HCl)

Compared to air-firing conditions, HCl emissions are particularly promoted during oxy-fuel combustion due to enhanced metal vaporization and chlorination achieved by flue gas recirculation [14]. The results depicted in Figure 8a corroborate the latter assertion. The specific HCl emissions at oxy-fuel conditions were over three times higher than those measured during the air-firing experiment, which is in line with the results reported by other authors [2]. Besides, the results depicted in Figure 8a indicate that excess oxygen (i.e., stoichiometric ratio) does not pose a substantial effect on HCl, mainly because of the fact that HCl is not an oxidation product.

The influence of temperature on HCl is presented in Figure 8b. According to Hou et al., elevated HCl concentration with temperature might be expected as a result of the increased gas partial pressure of metal chlorides [12]. However, there is a sharp decrease in  $y_{HCl}$  in the range between 871-880 °C that can be attributed to a decreased availability of SO<sub>2</sub> to form HCl in combination with the ability of CaO to absorb HCl under conditions typical for fluidized bed combustors [32].

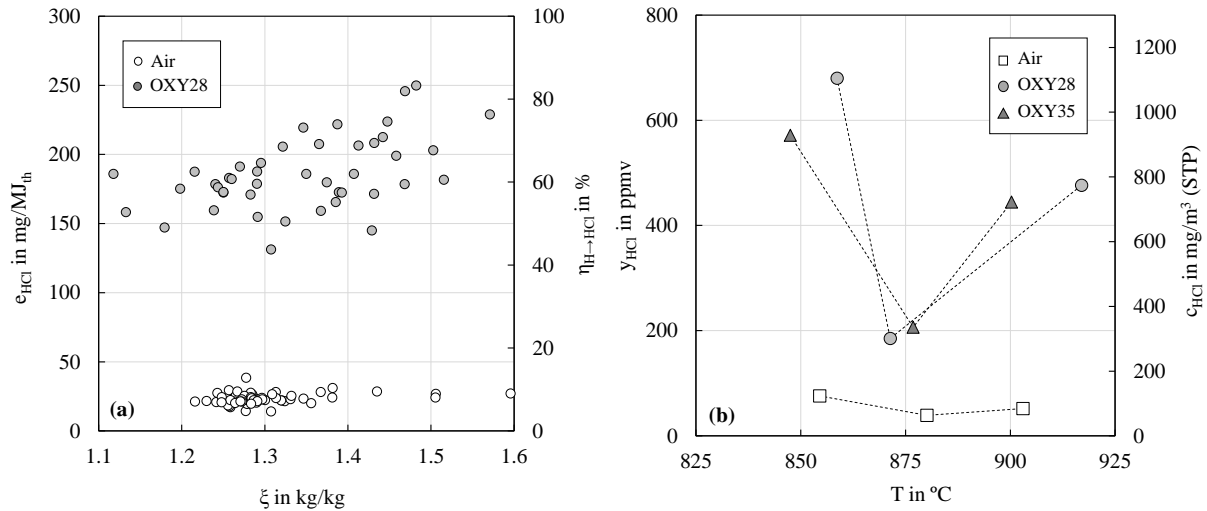


**Figure 8.** (a) HCl emission factor ( $e_{HCl}$ ) and fuel-H to HCl ratio ( $\eta_{H \rightarrow HCl}$ ) vs stoichiometric oxygen-to-fuel ratio ( $\xi$ ). (b) HCl concentration ( $y_{HCl}$ ,  $c_{HCl}$ ) vs reactor temperature ( $T$ ) [20]

## 4.2 Hydrodynamic behavior

Figure 9 introduces the temperature and pressure profiles of the 200 kW<sub>th</sub> oxy-fuel reactor during the conducted air-firing and oxy-fuel tests at a reference temperature of 880 °C.

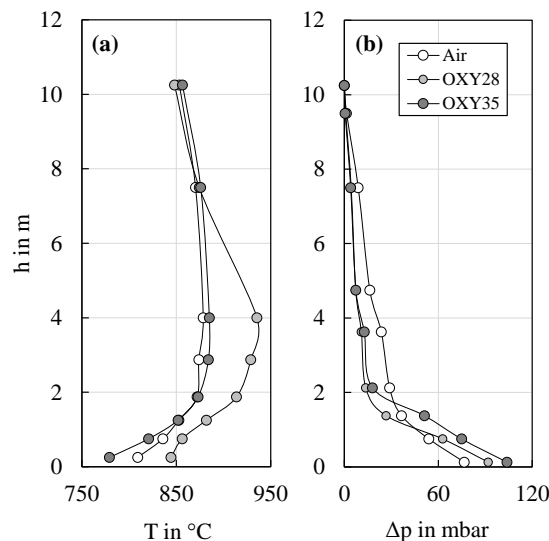


**Figure 9.** Temperature ( $T$ ) (a) and pressure ( $\Delta p$ ) (b) profiles along reactor height ( $h$ ) at a reference boiler temperature of 880 °C [20]



Overall, the furnace temperature evolution in the three experiments fell into the typical pattern described by a CFB combustor. This is characterized by stable temperatures in the upper part and a gradual temperature increase in the bottom region.

While all three experiments indicated a similar temperature behavior in the upper part, the bottom section of the reactor introduced a distinct pattern at the OXY28 case. Please note that the riser temperature was controlled using a fluidized bed top heat exchanger during the latter test. Due to the limited length of the cooling rods (of approx. 5 m), the heat exchanger could only accommodate temperature fluctuations occurring in the upper half of the reactor. In consequence, the bottom-middle section of the riser experienced enhanced combustion conditions (up to 936 °C). This operation mode was maintained for several hours, although it ultimately led to bed material sintering and agglomeration issues.

As for OXY35, a different approach was followed. Aiming at simulating a real fluidized bed cooler, the CFB reactor was coupled to a bubbling fluidized bed (BFB) reactor, setting the required process conditions to ensure smooth operation of the CFB reactor. For a detailed description of the proposed BFB-CFB reactor coupling please refer elsewhere [11,19]. As can be observed, the temperature distribution during OXY35 was very similar to the one obtained during air combustion conditions. This latter finding indicates that the advantages of increased inlet oxygen concentrations can be attained at the 200 kW<sub>th</sub> facility, providing that a uniform and sufficient cooling duty over the whole reaction height is guaranteed.

Besides, the pressure profile described by the CFB reactor was similar in all investigated cases. Figure 9 displays a shaped curve in the bottom region with an almost linear gradient in the riser, indicating a uniform distribution of the bed inventory along with the reactor height. Minor differences were attained in the bottom section of the reactor (i.e., up to 2 m). While a pressure drop of 77 mbar was measured during air-firing conditions, differences up to 104 mbar were obtained under oxy-fuel combustion. With negligible differences in the solid bed inventory, the latter effect can be explained through the reduction in total flue gas flow with respect to air-firing.

### 4.3 Operation at increased oxy-fuel levels

Within a next experimental phase, the inlet O<sub>2</sub> concentration was increased so as to investigate enhanced oxy-fuel operation conditions. Volume concentrations of up to 45 vol% were successfully demonstrated for about 8 hours of stable operation, yielding CO<sub>2</sub> concentrations up to 95 vol% at boiler outlet (see Figure 10). Please note that the increased excess oxygen level attained during test was required so as to ensure adequate fuel burnout within the system. Thanks to the homogeneous combustion conditions, no temperature hot spots or bed agglomeration issues were detected.

In line with the results published by other authors [11,19], the results obtained in this study indicate a linear behavior of inlet oxygen with the amount of recirculated flue gas (see Figure 11). Please recall that slight fluctuations in let inlet concentration are ascribed to changes in the excess level caused by fuel composition and homogeneity issues. In any case, the temperature distribution attained in the experiments was homogeneous, validating the proposed modification of utilizing a BFB reactor as a fluidized bed cooling system. Although higher oxy-fuel conditions might still be attainable with the suggested configuration, their investigation was outside this work's scope.

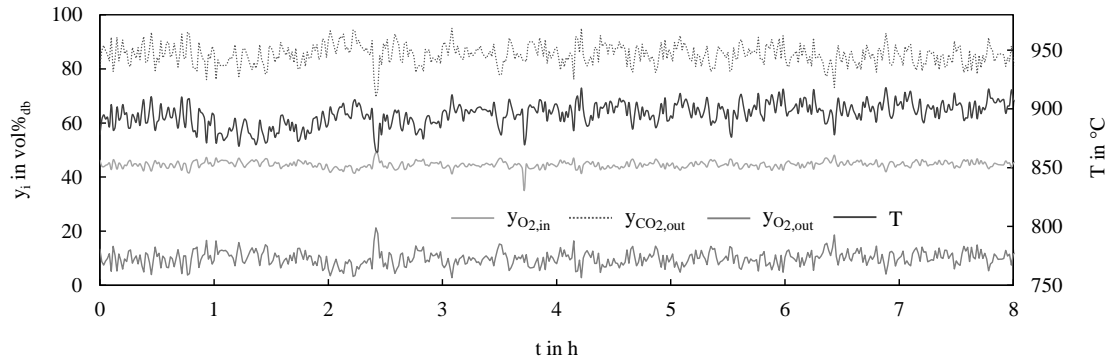


**Figure 10.** Demonstration of increased oxy-fuel long-term operation (45 vol% O<sub>2</sub> at reactor inlet)

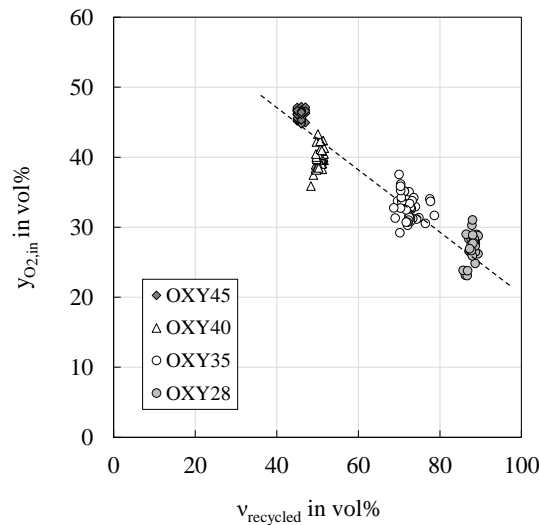


**Figure 11.** Inlet O<sub>2</sub> concentration vs fraction of recirculated gas

The results introduced in this deliverable demonstrate the viability of employing a CFB combustor for the combustion of low-grade fuels, achieving stable hydrodynamic conditions both during air and oxy-fuel firing conditions. Particularly at oxy-fuel conditions, the riser temperature distribution has played a major role in the stability of the system. The results included in this report have shown that temperatures below 930 °C are required in the bottom section to avoid any risks associated with bed material sintering and agglomeration.

## 5 Conclusions

This deliverable has analyzed the combustion behavior of SRF in a 200 kW<sub>th</sub> CFB combustion facility operated under industrially relevant process conditions (TRL6). Dedicated investigations on the influence of temperature and combustion atmosphere have been devoted to characterizing the process in terms of gas pollutant formation and hydrodynamic stability.

Compared to air-firing conditions, the volume concentration of NO<sub>x</sub> significantly increased during oxy-fuel operation (by about 50%). At the same time, fuel-specific NO<sub>x</sub> emissions decreased because of the absence of airborne nitrogen in combination with the reduced total gas volume flow. Besides, the process temperature posed a mild effect on the volume concentration of NO<sub>x</sub>, under the premise that temperature was homogeneously distributed along with the reactor height.

The concentration of SO<sub>2</sub> was particularly influenced by the presence of calcium-containing species in the fuel ash (by about 0.23 kg/kg) and was strongly inhibited at specific flue gas desulfurization temperatures (i.e., 871-880 °C).

HCl emissions showed to be mainly promoted during oxy-fuel combustion due to enhanced metal vaporization and chlorination achieved by flue gas recirculation. Similar to  $y_{SO_2}$ , the concentration of HCl showed to decrease within the temperature window of 871-880 °C due to the reduced availability of SO<sub>2</sub> required for alkali sulfation in combination with the ability of calcium-containing ash species to absorb HCl.

A smooth temperature profile in the riser proved to be essential to allow for stable investigation of increased oxy-fuel cases. The pressure differences across the riser were comparable in all tests, with slightly higher pressure drops during oxy-fuel combustion due to the reduced total gas throughput.

The results included in this study contribute to a better understanding of the fundamental oxy-fuel knowledge with alternative fuels and may serve to guide future process design and scale-up.

## Acknowledgements

The authors gratefully acknowledge the financial support by the German Federal Ministry of Economic Affairs and Climate Action, BMWK, (Grant No. 03EE5020) and the cooperation and support by the NEWEST-CCUS (Project No. 299683) project partners.

## References

- [1] 13. BImSchV. "Verordnung über Großfeuerungs-, Gasturbinen- und Verbrennungsmotoranlagen vom 2. Mai 2013 (BGBl. I S. 1021, 1023, 3754), die zuletzt durch Artikel 108 der Verordnung vom 19. Juni 2020 (BGBl. I S. 132) geändert worden ist". Berlin, Germany, 2013: Bundesministerium der Justiz und für Verbraucherschutz. Bundesamt für Justiz.
- [2] Allgurén T, Andersson K. Chemical Interactions between Potassium, Sulfur, Chlorine, and Carbon Monoxide in Air and Oxy-fuel Atmospheres. *Energy Fuels* 2020;34(1):900–6. <https://doi.org/10.1021/acs.energyfuels.9b03078>.
- [3] Bui M, Fajardy M, Dowell N. Thermodynamic Evaluation of Carbon Negative Power Generation: Bio-energy CCS (BECCS). *Energy Procedia* 2017;114:6010–20. <https://doi.org/10.1016/j.egypro.2017.03.1736>.
- [4] Chang KK, Flagan RC, Gavalas GR, Sharma PK. Combustion of calcium-exchanged coals. *Fuel* 1986;65(1):75–80. [https://doi.org/10.1016/0016-2361\(86\)90145-6](https://doi.org/10.1016/0016-2361(86)90145-6).
- [5] Díez LI, Lupiáñez C, Guedea I, Bolea I, Romeo LM. Anthracite oxy-combustion characteristics in a 90 kW<sub>th</sub> fluidized bed reactor. *Fuel Process Technol* 2015;139:196–203. <https://doi.org/10.1016/j.fuproc.2015.07.021>.
- [6] Ditaranto M, Becidan M, Stuen J. Opportunities for CO<sub>2</sub> Capture in the Waste-to-Energy Sector. *Waste Management*. Thomé-Kozmiensky Verlag GmbH. 2019;9:319–328.
- [7] Elorf A, Sarh B. Excess air ratio effects on flow and combustion characteristics of pulverized biomass (olive cake). *Case Stud Therm Eng* 2019;13:100367. <https://doi.org/10.1016/j.csite.2018.100367>.

- [8] European Commission. The role of waste-to-energy in the circular economy. Brussels, Belgium; 2017.
- [9] Gough C, Upham P. Biomass energy with carbon capture and storage (BECCS or Bio-CCS). *Greenhouse Gas Sci Technol* 2011;1(4):324–34. <https://doi.org/10.1002/ghg.34>.
- [10] Hofbauer G, Beisheim T, Dieter H, Scheffknecht G. Experiences from Oxy-fuel Combustion of Bituminous Coal in a 150 kW<sub>th</sub> Circulating Fluidized Bed Pilot Facility. *Energy Procedia* 2014;51:24–30. <https://doi.org/10.1016/j.egypro.2014.07.003>.
- [11] Hornberger M, Moreno J, Schmid M, Scheffknecht G. Experimental investigation of the calcination reactor in a tail-end calcium looping configuration for CO<sub>2</sub> capture from cement plants. *Fuel* 2021;284:118927. <https://doi.org/10.1016/j.fuel.2020.118927>.
- [12] Hou H, Li S, Lu Q. Gaseous Emission of Monocombustion of Sewage Sludge in a Circulating Fluidized Bed. *Ind Eng Chem Res* 2013;52(16):5556–62. <https://doi.org/10.1021/ie4002537>.
- [13] Ikeda M, Toporov D, Christ D, Stadler H, Förster M, Kneer R. Trends in NO<sub>x</sub> Emissions during Pulverized Fuel Oxy-fuel Combustion. *Energy Fuels* 2012;26(6):3141–9. <https://doi.org/10.1021/ef201785m>.
- [14] Jiao F, Chen J, Zhang L, Wei Y, Ninomiya Y, Bhattacharya S et al. Ash partitioning during the oxy-fuel combustion of lignite and its dependence on the recirculation of flue gas impurities (H<sub>2</sub>O, HCl and SO<sub>2</sub>). *Fuel* 2011;90(6):2207–16. <https://doi.org/10.1016/j.fuel.2011.02.016>.
- [15] Krzywanski J, Czakiert T, Shimizu T, Majchrzak-K. I, Shimazaki Y, Zylka A et al. NO<sub>x</sub> Emissions from Regenerator of Calcium Looping Process. *Energy Fuels* 2018;32(5):6355–62. <https://doi.org/10.1021/acs.energyfuels.8b00944>.
- [16] Liu Q, Zhong W, Yu H, Tang R, Yu A. Experimental Studies on the Emission of Gaseous Pollutants in an Oxy-Fuel-Fluidized Bed with the Cofiring of Coal and Biomass Waste Fuels. *Energy Fuels* 2020;34(6):7373–87. <https://doi.org/10.1021/acs.energyfuels.0c01061>.
- [17] Lupiáñez C, Mayoral MC, Díez LI, Pueyo E, Espatolero S, Andrés JM. The role of limestone during fluidized bed oxy-combustion of coal and biomass. *Appl Energy* 2016;184:670–80. <https://doi.org/10.1016/j.apenergy.2016.11.018>.
- [18] Moreno J, Hornberger M, Schmid M, Scheffknecht G. Oxy-Fuel Combustion of Hard Coal, Wheat Straw, and Solid Recovered Fuel in a 200 kW<sub>th</sub> Calcium Looping CFB Calciner. *Energies* 2021;14(8):2162. <https://doi.org/10.3390/en14082162>.
- [19] Moreno J, Hornberger M, Schmid M, Scheffknecht G. Part-Load Operation of a Novel Calcium Looping System for Flexible CO<sub>2</sub> Capture in Coal-Fired Power Plants. *Ind Eng Chem Res* 2021. <https://doi.org/10.1021/acs.iecr.1c00155>.
- [20] Moreno J, Schmid M, Scharr S, Scheffknecht G. Oxy-Combustion of Solid Recovered Fuel in a Semi-Industrial CFB Reactor: On the Implications of Gas Atmosphere and Combustion Temperature. *ACS Omega* 2022;7(10):8950–9. <https://doi.org/10.1021/acsomega.1c07334>.
- [21] Nowak P. Combustion of biomass and solid recovered fuels on the grate. Universität Stuttgart 2019. <https://doi.org/10.18419/opus-10749>.

- [22] Pang L, Shao Y, Zhong W, Gong Z, Liu H. Experimental study of NO<sub>x</sub> emissions in a 30 kW<sub>th</sub> pressurized oxy-coal fluidized bed combustor. *Energy* 2020;194:116756. <https://doi.org/10.1016/j.energy.2019.116756>.
- [23] Pikkarainen T, Saastamoinen J, Saastamoinen H, Leino T, Tourunen A. Development of 2<sup>nd</sup> Generation Oxyfuel CFB Technology – Small Scale Combustion Experiments and Model Development Under High Oxygen Concentrations. *Energy Procedia* 2014;63:372–85. <https://doi.org/10.1016/j.egypro.2014.11.040>.
- [24] RAL-GZ 724. Sekundärbrennstoffe - Gütesicherung. Münster, Germany, 2012: RAL Deutsches Institut für Gütesicherung und Kennzeichnung e. V.
- [25] Shah M, Degenstein N, Zanfir M, Kumar R, Bugayong J, Burgers K. Near zero emissions oxy-combustion CO<sub>2</sub> purification technology. *Energy Procedia* 2011;4:988–95. <https://doi.org/10.1016/j.egypro.2011.01.146>.
- [26] Spliethoff H. *Power Generation from Solid Fuels*. Berlin, Germany: Springer-Verlag; 2010.
- [27] Spörl R, Maier J, Scheffknecht G. Sulphur Oxide Emissions from Dust-fired Oxy-fuel Combustion of Coal. *Energy Procedia* 2013;37:1435–47. <https://doi.org/10.1016/j.egypro.2013.06.019>.
- [28] Stanger R, Wall T, Spörl R, Paneru M, Grathwohl S, Weidmann M et al. Oxyfuel combustion for CO<sub>2</sub> capture in power plants. *Int J Greenh Gas Control* 2015;40F:55–125. <https://doi.org/10.1016/j.ijggc.2015.06.010>.
- [29] Tan Y, Jia L, Wu Y, Anthony EJ. Experiences and results on a 0.8 MW<sub>th</sub> oxy-fuel operation pilot-scale circulating fluidized bed. *Appl Energy* 2012;92:343–7. <https://doi.org/10.1016/j.apenergy.2011.11.037>.
- [30] United Nations Treaty Collection. *The Paris Agreement: Chapter XXVII 7 d*. Paris, France; 2015.
- [31] Wienchol P, Szlęk A, Ditaranto M. Waste-to-energy technology integrated with carbon capture. Challenges and opportunities. *Energy* 2020;198:117352. <https://doi.org/10.1016/j.energy.2020.117352>.
- [32] Xie W, Liu K, Pan W-P, Riley JT. Interaction between emissions of SO<sub>2</sub> and HCl in fluidized bed combustors. *Fuel* 1999;78(12):1425–36. [https://doi.org/10.1016/S0016-2361\(99\)00070-8](https://doi.org/10.1016/S0016-2361(99)00070-8).